Broadband and highly efficient quadratic interactions in double-slot lithium niobate waveguides through phase matching

Jun-long Kou,[1] Qin Wang,[1] Zi-yan Yu,[1] Fei Xu,[1,*] and Yan-qing Lu[1,2]

[1]*College of Engineering and Applied Sciences and National Laboratory of Solid State Microstructures, Nanjing University, Nanjing 210093, China*

[2]*e-mail: yqlu@nju.edu.cn*

**Corresponding author: feixu@nju.edu.cn*

Received April 4, 2011; revised June 5, 2011; accepted June 6, 2011; posted June 7, 2011 (Doc. ID 145349); published June 30, 2011

We propose and study in detail a phase-matched quadratic optical interaction in a realizable 2D double-slot lithium niobate (LN) waveguide. As opposed to the single-slot waveguide, the field can be well confined in the nanometric nonlinear material, and it is also more flexible for birefringence and dispersion design. The proposed compact double-slot structure could not only achieve form birefringence phase matching but also effectively enhance the modal overlap integral and expand the working wavelength. The calculated results on second harmonic generation show an extremely large bandwidth of ~40 nm. The modal overlap integral up to 0.035 $W^{3/2}/V$ can be realized by optimizing the waveguide geometry, and it is much better than previous results on single-slot waveguides. Its temperature dependence is low—around 25 °C. The geometry is practical considering the current micromachining technique of LN.

OCIS codes: 190.4410, 130.3120.

Quadratic optical interactions have been intensively studied considering frequency generation, parametric amplification and oscillation, signal processing, and quantum optics [1–3]. The conversion efficiency of these interactions relates to the pump intensity, spatiotemporal overlap of interacting waves, and momentum conservation or phase-velocity matching. In bulk crystal materials, phase matching (PM) is the major issue, and several methods have been suggested and demonstrated, including birefringence PM by angle or temperature tuning, quasi-PM by bonding of several materials [4], and ferroelectric poling [5]. In optical waveguides, form birefringence PM by geometry-related birefringence is a very efficient method, even for isotropic materials such as cubic semiconductors. But another issue on the guided mode is spatiotemporal overlap, which also has to be considered carefully [6]. As the key element of large-scale photonic integrated circuits, nanoscale high-index-contrast 2D waveguides with ultrasmall guided mode areas are intensively investigated for their nonlinear applications with different structures and materials, including cubic silicon and quadratic lithium niobate (LN). LN is a unique ferroelectric material with perfect acoustic-optical, electro-optical, and nonlinear properties in a large transparency range (0.39–5 μm), and it is readily available in large high-quality single-crystal wafers. However, it is still challenging to achieve PM with high efficiency in a nanoscale LN-rib waveguide with a reasonable structure, substrate, and process. Thanks to the recent breakthroughs in micromachining techniques, the lossless slot waveguide composed of a narrow low-index slot sandwiched between two high-index materials has attracted more and more attention for nonlinear applications due to its high field confinement and controllable birefringence and dispersion tailoring [7–9]. Form birefringence PM based on the single-slot waveguide has only been theoretically discussed for semiconductors ($Al_{0.3}Ga_{0.7}As$) with an unpractical assumption that the waveguide is free-standing, and the field modal overlap is very small because of the highly confined field in the air gap [10]. So far there has been little work done on birefringence PM in the nanoscale 2D LN waveguide.

In this Letter, we propose and theoretically investigate the highly efficient and broadband quadratic interaction in a realizable double-slot LN waveguide. Compared with the previous single-slot waveguide, our design can confine more of the light field in the nanometric nonlinear material because of an extra slot being introduced. Another benefit of the waveguide is more flexibility in birefringence and dispersion design. Attributed to the unique geometry, the proposed double-slot structure could achieve form birefringence PM for any wavelength while effectively enhancing the modal overlap and expanding the working wavelength. An extremely large bandwidth (~40 nm) and modal overlap integral (~0.035 $W^{3/2}/V$) can be realized by optimizing the waveguide geometry according to our calculated results on second harmonic generation (SHG) at a fundamental wavelength of 1600 nm. And it has low temperature dependence of around 25 °C. The geometry is realizable with the current micromachining technique of silicon and LN [11–14]. Attributed to the high conversion efficiency, broad bandwidth, and high tolerance to temperature, the intriguing double-slot LN waveguide opens up a wealth of possibilities for the quadratic parametric process for future large-scale nonlinear phonic integrated circuits in the visible and IR ranges.

We consider the basic structure sketched in Fig. 1. It is assumed that the LN guiding layer is set on top of a low-index substrate film (500 nm thick silica is considered here) denoted as the red (bottom) part, and all the parts are exposed in air for simplicity. The waveguide is a symmetric structure when viewed along the x axis, which means the two slots are identical in size. The geometric parameters of the waveguide are presented in Fig. 1. The incident light propagates along the x axis so that the

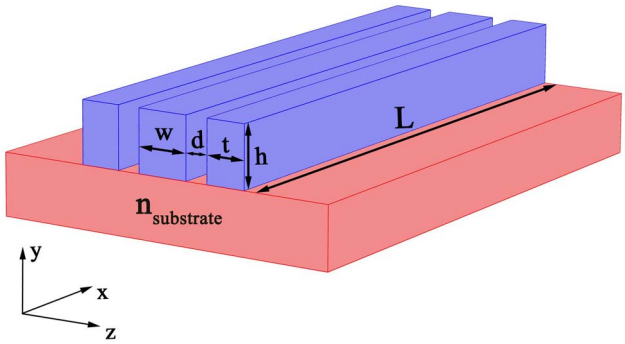

Fig. 1. (Color online) Schematic of the double-slot waveguide with air voids: the blue (top) and red (bottom) parts are the LN and low-index substrate, respectively.

quasi-TM fundamental wave (FW) could be coupled to the quasi-TE second harmonic (SH) wave through the quadratic nonlinear susceptibility d_{31}. All the calculation work is done by using a full-vectorial finite-element analysis solver. This kind of structure is realizable with recent advances in LN waveguide fabrications [11–14]. As illustrated in [11,14], the thin LN wafer with a low-index substrate is prepared using the ion slicing and wafer bonding technique. The structure proposed here can thus be fabricated by selectively removing part of the LN using the focused ion beam method or deep-UV photolithography.

Figure 2 displays the calculated electric field distribution of the quasi-TM FW and the quasi-TE SH of the first-order bounded mode at a fundamental wavelength of 1600 nm. As can be seen, different from the single-slot waveguide or the high-index-contrast rib waveguide, the majority of the electric field remains in the central nanometric LN rib but not in the voids. It results in a very large modal overlap integral between the FW and SH, thus leading to relatively high conversion efficiency.

In bulk LN, the original mismatch of the cross-polarized FW and SH Δ_{eff} ($\Delta_{\text{eff}} = n_z^{\text{SH}} - n_y^{\text{FW}}$) does not equal zero. In a double-slot LN waveguide, the structure has a different influence on n_z and n_y, which are the effective indices of the fundamental mode polarized along the z and y axes. For the excited z-polarized mode, there is a large discontinuity of the electric field occurred along the air/LN interface, and the effective index n_z and dispersion are much different from bulk LN. On the contrary, for the excited y-polarized mode, most of the light is well confined in the nonair central part of the guiding layer. There is a relatively smaller effect resulting

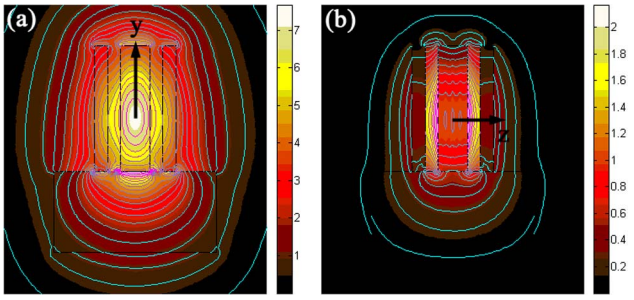

Fig. 2. (Color online) Electric field distribution of the (a) quasi-TM FW at 1600 nm and (b) quasi-TE SH at 800 nm, with black arrows denoting the electric field direction: $w = 180$ nm, $d = 80$ nm, $t = 80$ nm, and $h = 774$ nm.

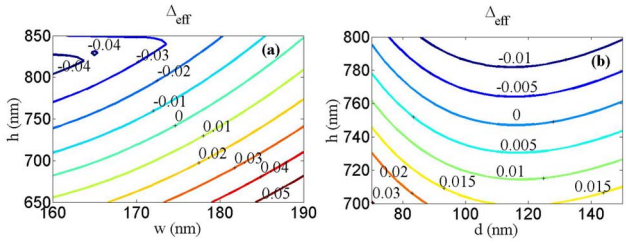

Fig. 3. (Color online) Mapping of Δ_{eff} with respect to (a) w and h at $d = 80$ nm, $t = 80$ nm and (b) d and h at $w = 180$ nm, $t = 80$ nm. The PM condition is achieved with the line $\Delta_{\text{eff}} = 0$.

from the changing of geometry. The effective index n_y and its dispersion, thus, is more similar with bulk LN. By tuning the geometric parameters, this modal dispersion compensates the material dispersion and makes PM, i.e., $\Delta_{\text{eff}} = 0$ possible.

In order to find the PM condition of SHG with the structure, we calculate the effective indices of the cross-polarized FW and SH by mapping two geometric parameters in different conditions. Part of the results is shown in Fig. 3, in which the PM condition is denoted as the line $\Delta_{\text{eff}} = 0$. PM can be achieved over a wide range of realizable geometric parameters. Taking the benefit of the flexible structure and large tuning range of effective index and dispersion, this method and procedure can be applied for arbitrary wavelength in the visible and IR.

In order to investigate the properties of the modal overlap integral and conversion bandwidth, a waveguide of unity length $L = 1$ mm is assumed. The modal overlap integral Γ is expressed as

$$\Gamma = \iint_S E_z^{\text{SH}}(y,z)[E_y^{\text{FW}}(y,z)]^2 d_{\text{eff}}(y,z)\mathrm{d}y\mathrm{d}z, \qquad (1)$$

where $d_{\text{eff}}(x,y)$ is the spatial distribution of the effective nonlinear susceptibility coupling a y-polarized FW to a z-polarized SH. $d_{\text{eff}}(x,y) = d_{31}$ within the LN region and $d_{\text{eff}}(x,y) = 0$ elsewhere. $E(x,y)$ represents the electric field amplitude of the transverse waveguide modes normalized to yield unit power at the two wavelengths (i.e., $P_x = \frac{1}{4}\iint(\vec{E}\times\vec{H}^* + \vec{H}\times\vec{E}^*)\cdot\vec{e}_x\mathrm{d}y\mathrm{d}z = 1$). The normalized conversion efficiency in the undepleted-pump limit is given by

$$\eta_{\text{norm}} \propto [\Gamma \times \text{sinc}(\Delta\beta \times L/2)]^2, \qquad (2)$$

where the phase mismatch is $\Delta\beta = 4\Pi\Delta_{\text{eff}}/\lambda$ and λ is the fundamental wavelength in free space.

Figures 4(a) and 4(b) graph the modal overlap integral and normalized conversion efficiency as a function of the fundamental wavelength (phase matched and phase mismatched) under different geometric conditions. The PM condition is satisfied exactly at the FW of 1600 nm under all these geometry conditions.

As can be deduced from Fig. 4(a), the modal overlap integral increases when a shorter fundamental wavelength is used. This is because the guiding layer has more ability to well confine the light field in the middle LN medium. The modal overlap integral is 1 order of magnitude

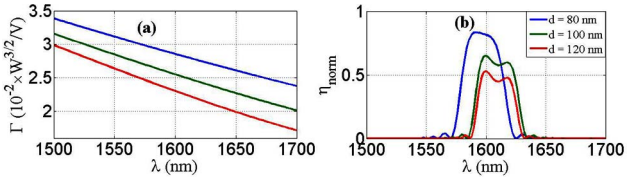

Fig. 4. (Color online) (a) Modal overlap integral and (b) normalized conversion efficiency as a function of the fundamental wavelength. The PM point is tuned to 1600 nm with three set of different geometric parameters by varying d and h. The waveguide is set to be 1 mm in length.

higher than previous results of single-slot waveguide in highly nonlinearity semiconductors [10].

As the blue (top) curve in Fig. 4(b) indicates, a broad bandwidth up to 40 nm can be obtained, 1 order of magnitude wider than that of the first-order quasi-PM in bulk periodically poled LN. However, the highest conversion efficiency is not located at the PM point, i.e., 1600 nm. This can be explained by the fact that two factors influence the efficiency simultaneously. The first is the sinc function $\mathrm{sinc}^2(\Delta\beta L/2)$, which is related to the phase mismatch $\Delta\beta$. The second is the modal overlap integral, which leads to the deviation of the highest conversion efficiency from the PM point, clearly shown in Fig. 4(a). As the wavelength deviates far from 1600 nm, phase mismatching increases, and as a result, the conversion efficiency decreases. The ripples in the figure are due to the sinc function. We also calculate the bandwidth with two other geometric parameters, the green (middle) and red (bottom) curves in Fig. 4(b). As d increases, not only does the conversion bandwidth becomes narrow, but also the conversion efficiency decreases. For technical consideration, waveguides with smaller d are not studied here. In a word, by optimizing the waveguide geometry, a high conversion efficiency and broad bandwidth could be achieved in SHG.

Temperature tolerance is one key issue in practical applications of nonlinear optics. In bulk nonlinear crystals, a highly precise external temperature controller is employed to achieve PM and stable output power. However, in large-scale photonic integrated circuits, it is impossible to control the temperature of each element individually.

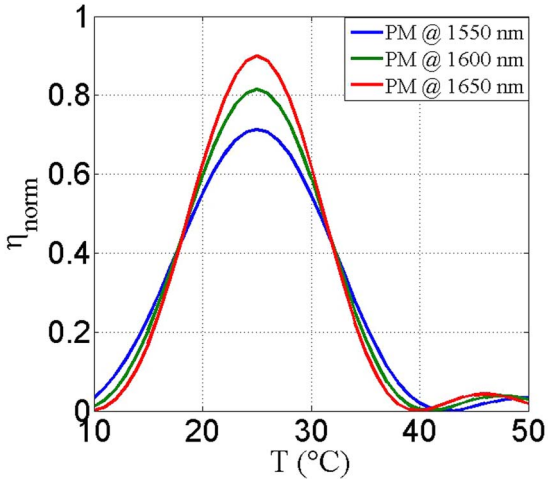

Fig. 5. (Color online) Temperature dependent normalized SHG conversion efficiency at different pumping wavelength. The blue (bottom), green (middle), and red (top) curves are obtained when $w = 170$, 180, and 190 nm, respectively.

Thus for a nanometric waveguide in photonic integrated circuits, large temperature tolerance especially at room temperature is important and necessary. Here the double-slot structure provides us with more freedom and possibilities to engineer the temperature dependence.

We study the temperature dependence of the normalized conversion efficiency. The three lines in Fig. 5 are plotted under different geometric parameters in order to meet the PM condition at different fundamental wavelengths. The temperature range of ~15 °C is obtained when η_{norm} drops to half of its peak value at room temperature. It is enough for practical applications in large-scale photonic integrated circuits. And by incorporating some polymer in our design, temperature tolerance could be further improved [15].

We have carried out a design of a realizable double-slot LN-based waveguide and numerically investigated its nonlinear properties associated with SHG. PM is achieved over a wide range of geometric parameters, and broadband SHG can be realized by utilizing the dispersion character provided. Benefiting from the unique geometry, the design could both achieve form birefringence PM for any wavelength and effectively enhance the modal overlap and expand the working wavelength. These are much larger than previous results on single-slot waveguides. The double-slot LN-based waveguide shows significant potential for practical applications in large-scale photonic integrated circuits at room temperature given the merit of its flexible design, large conversion efficiency, high bandwidth, low temperature dependence, and fabrication without spatially periodically poling.

This work is supported by the National 973 Program under contracts 2010CB327800 and 2011CBA00205.

References

1. A. D. Boardman, *Advanced Photonics With Second-Order Optically Nonlinear Processes* (Kluwer, 1999).
2. J. A. Armstrong, N. Bloembergen, J. Ducuing, and P. S. Pershan, Phys. Rev. **127**, 1918 (1962).
3. P. A. Franken, A. E. Hill, C. W. Peters, and G. Weinreich, Phys. Rev. Lett. **7**, 118 (1961).
4. M. J. Missey, V. Dominic, L. E. Myers, and Robert C. Eckardt, Opt. Lett. **23**, 664 (1998).
5. L. E. Myers and W. R. Bosenberg, J. Quant. Electron. **33**, 1663 (1997).
6. A. Fiore, V. Berger, E. Rosencher, P. Bravetti, and J. Nagle, Nature **391**, 463 (1998).
7. R. Sun, P. Dong, N.-n. Feng, C.-y. Hong, J. Michel, M. Lipson, and L. Kimerling, Opt. Express **15**, 17967 (2007).
8. A. Khanna, A. Saynatjoki, A. Tervonen, R. A. Norwood, and S. Honkanen, Appl. Opt. **49**, 5321 (2010).
9. V. R. Almeida, Q. Xu, C. A. Barrios, R. A. Norwood, and S. Honkanen, Opt. Lett. **29**, 1209 (2004).
10. A. Di Falco, C. Conti, and G. Assanto, Opt. Lett. **31**, 3146 (2006).
11. A. Guarino, G. Poberaj, D. Rezzonico, R. Degl'Innocenti, and P. Gunter, Nat. Photon. **1**, 407 (2007).
12. S.-H. Yang, M. L. Cooper, P. R. Bandaru, and S. Mookherjea, Opt. Express **16**, 8306 (2008).
13. A. Majkic, M. Koechlin, G. Poberaj, and P. Gunter, Opt. Express **16**, 8769 (2008).
14. F. Sulser, G. Poberaj, M. Koechlin, and P. Gunter, Opt. Express **17**, 20291 (2009).
15. J.-M. Lee, D.-J. Kim, G.-H. Kim, O. K. Kwon, K.-J. Kim, and G. Kim, Opt. Express **16**, 1645 (2008).